IP-2 1215

ASAT

MILITARY TECHNICAL COLLEGE
CAIRO - EGYPT

COMPUTERIZED TOMOGRAPHY: A TOOL IN FLUID FLOW AND COMBUSTION DIAGNOSTICS

H.YAKOUT *

ABSTRACT

Computerized axial tomographic reconstruction technique (CAT) has been originally developed for X-ray medical applications. The technique is widely used to obtain cross-sectional pictures of living bodies, mapping not only their structures, but also some of their physiological functions. This technique is successfully extended to map chemical species concentration and temperature fields across reacting and non-reacting flows. The method has the capability of high-speed (real-time), three-dimensional reconstruction of laminar and turbulent flow fields.

In our paper, we present and review the convolution algorithm for tomographic reconstruction of a three-dimensional field from a set of corresponding two-demensional projections. The algorithm involves parallel beams geometry and multiangular laser-based absorption measurements. The effects of the choice of filtering functions together with the required number of viewing angles on the algorithm performance are demonstrated with the aid of simulation results of two axisymmetric functions similar to the profiles in fluid flow and combustion processes.

* Assistant Professor, Dept. of Weapons and Ammunition, Military Technical College, Cairo, Egypt.

SECOND A.S.A.T. CONFERENCE
21 - 23 April 1987 , CAIRO

INTRODUCTION

Nowadays, with the advent of lasers and rapid data collection techniques, laser-based nonintrusive optical diagnostic techniques are the major investigative tools in fluid flowfields and combustion processes. These techniques make use of the dependence of the flow's optical properties on its thermodynamic properties. They are capable of providing not only excellent time response as well as space resolution (instantaneous point measurement), but also overcome all limitations of the intrusive probing techniques.

Nonintrusive optical techniques have seen a rapid rate of development in the last fifteen years. Recent reviews [1-5] discuss the increasing practical availability of such techniques in measuring velocity, temperature, density and species concentration fields. They are based on light scattering, interferometery, fluorescence, emission and absorption processes. Among these techniques are Rayleigh scattering, Mie scattering, Raman scattering in both linear and nonlinear forms, laser induced fluorescence and computerized tomography. Each of these methods has a range of applications where it is superior to others, but non carries a universal applicability. Thus a need to select the appropriate method from this complete set exists.

Computerized axial tomographic reconstruction technique (CAT) based on absorption process has been originally proposed and developed for radio-astronomy and medical radiology [6-9]. The mathematical foundations of tomography had been established by Radon [6], but Bracewell [7] was the first to obtain practical reconstructions in the field of radio-astronomy. Image reconstruction in the area of medical applications was carried out by Cormack [8]. His results formed the basis for the development of medical CAT scanners. The first commercial scanner was designed in London by Hounsfield in 1970 [9]. Because of the substantial success of the technique in these fields, it was adapted by contributors from other fields such as fluid flow and combustic diagnostics field [10-15], meteorology and oceanography [16-17].

The tomographic methods for retrieving the property field have been developed in two different directions: iterative algebraic reconstruction (ART) techniques [18] and Fourier transform (FT) techniques. Ramachandran and Lakshminarayanan [19] proposed the use of convolution instead of FT technique. Their approach has higher speed of computation because it involves only 1-D summation instead of doing 2-D FTs. They introduced a specific weighting function. This function was later treated in details by Shepp and Logan [20], and by Kwoh and others [21].

The applications of laser -based tomography to fluid flow and combustion diagnostics were recantly proposed by Goulard and Emmarman [10,11]. An advantage of the technique is that it relies on absorption properties of the flow chemical components, which posses much larger cross sections than any other optical processes. This improves the method ability to measure low concentrations and to track rapidly fluctuating signals. As in flow transition regions where mixing and combustion take place in coherent structure modes evolving at rates of the order of one KHz and more [22 ,23]. The corresponding disadvantage is that very few combustion molecules (CH_4, OH, CO... etc) have absorption lines in the optical range of available laser sources.

Studies in the field of combustion diagnostics utilized convolution tomographic algorithm with parallel beam geometry and modified Shepp -Logan filter function [10-15]. The specific choice of such filter was made because it provides both damping response to the cut-off frequency of the field to be retrieved and has low sensitivity to measuring noise [20]. In the present paper, we review the convolution algorithm adapted for fluid flow and combustion applications . Based on simulation studies, we investigate the appropriateness of other available digital filter functions. Also the effects of limited number of viewing angles on the performance of the algorithm are demonstrated.

CONVOLUTION ALGORITHM

The transmitted radiation in an absorption process is given by the Bouguer-Lambert-Beer low [24]

$$I_\nu = I_{\nu o} \exp\left[-\int_{-\infty}^{\infty} Q_{\nu i}\ N_i\ ds\right] \tag{1}$$

Application of absorption tomagraphic technique in combustion and fluid fow measurements (for point measurement of the property field) involves multiangular absorption measurements along M equally-spaced parallel beams at N equally-spaced angles [10-12]. The MxN data set is used to reconstruct the original concentration field, $Q_{\nu_i}\ N_i$. The temperature field can be rerieved by ratioing the intensity measurements taken at two neighbouring frequencies (Boltzmann's relation). The absorption along each beam in Eq. (1) can be rewritten as (see Fig.1).

$$P(r,\theta) = \int_{-\infty}^{\infty} F(x,y)\ ds \tag{2}$$

The multiangular technique is based on reconstructing the function, $F(x,y)$, from a set of its projections, $P(r,\theta)$. The convolution method developed by Ramachandran and Lakshminarayanan [19] will be summarized here. Although it is a FT approach, it does not require the evaluation of any transforms. The 1-D FT of Eq. (2) can be written as

$$\hat{P}_\theta(\omega) = \int_{-\infty}^{\infty} P(r,\theta) \exp(-i\omega r)\, dr$$

$$= \int_{-\infty}^{\infty}\int_{-\infty}^{\infty} F_\theta(r,s) \exp(-i\omega r)\, dr\, ds \tag{3}$$

Introducing the 2-D FT of the function $F_\theta(r,s)$, such that

$$\hat{F}_\theta(\omega,\eta) = \int_{-\infty}^{\infty}\int_{-\infty}^{\infty} F_\theta(r,s) \exp\left[-i\,(\omega r+\eta\, s)\right] dr\, ds \tag{4}$$

Comparing Eqs. (3) and (4), we can see that $\hat{P}_\theta(\omega) = \hat{F}_\theta(\omega,o)$, which is the central Slice Theorem, [25], see Fig.2. A 180 degree sweep of angle θ will yield all values of $F(\omega,\eta)$ in the frequency domain. The function $F(x,y)$ can be reconstructed as the inverse FT of the set of $\hat{P}_\theta(\omega)$ obtained by measurements . The inverse FT of Eq. (4) will be given as

$$F(x,y) = \frac{1}{(2\pi)^2} \int_o^{\pi}\int_{-\infty}^{\infty} \hat{P}_\theta(\omega)\,|\omega| \exp\left[i\,\omega\, r\right] d\omega\, d\theta \tag{5}$$

The $|\omega|$ comes from the Jacobian of coordinates transformation. By defining a function $\phi(r)$ such that its FT is given by $\hat{\phi}(\omega) = |\omega|$. From the convolution theorem [26], the inner integral of Eq. (5) can be evaluated as

$$V(r,\theta) = \int_{-\infty}^{\infty} P(\tau,\theta).\ \phi(r-\tau)\ d\tau \qquad (6)$$

and Eq. (5) will be re-arranged to have the form

$$F(x,y) = \frac{1}{2\pi} \int_{0}^{\pi} \int_{-\infty}^{\infty} P(\tau,\theta)\ \phi(r-\tau)\ d\tau\ d\theta \qquad (7)$$

Because $P(r,\theta)$ is known only in the sampled domain (discrete values), the integrals in Eq. (7) must be replaced by their discrete summations. The corresponding reconstruction approximate formula is given by

$$F(x,y) = \frac{a}{2N} \sum_{j=1}^{N} \sum_{k=-\infty}^{k=\infty} P(r_k,\theta_j).\ \phi(x\cos\theta_j + y\sin\theta_j - r_k) \qquad (8)$$

Accurate reconstruction of the property field, will depend on the proper choice of the sampling intervals (M and N). Nyquist sampling theorem [26], requires that the sampling rate has to satisfy the condition $S_r \geqslant 2\ \rho_{max}$ for unique recovery of the reconstructed function. Emmerman and others [13] discussed the conditions for proper choice of M and N. They require that $(4\ R\ \rho_{max})$ equally-spaced rays to be measured at $(2\pi\ R\ \rho_{max})$ eqally-spaced angles, are necessary for proper retrieval of the field function. If such criteria are not met, the reconstructed field will likely show effects due to aliasing [26]. Oversampling is unnecessary from theoretical point of view , but it can improve the reconstruction accuracy in the presence of noise [11, 20].

FILTER FUNCTIONS

Since the inverse FT of the function $|\omega|$ does not converge, the convolution algorithm (Eq. 8) will require that the FT of $\phi(r)$ satisfy the conditions $\hat{\phi}(\omega) \doteq |\omega|$ for $|\omega| \leqslant 2\pi\ \rho_{max}$, and slowly go to zero, $\hat{\phi}(\omega) = 0$, for $\omega > 2\pi\rho_{max}$. The choice of the approximate function $\hat{\phi}(\omega)$ will greatly affect the computational speed as well as the accuracy of the retrieved property field. Because the multiplication of two FTs in the frequency domain is consisdered as a filtering operation, the approximation $\hat{\phi}(\omega) \doteq |\omega|$ is called an $|\omega|$-filter, and its spatial response $\phi(r)$ is called a digital filter function.

There have been a number of filter functions generated for medical tomography [19-21], many of which are quite suitable for fluid flow and combustion applications. The frequency responses of these particular filter functions are defined in Table 1. They are assumed to be linear in distances between parallel rays; this will result in large saving of computational time [19] . Using linear interpolation of a filter function is equivalent to the convolution of its spatial response with a triangular function of suitable size. This means to multiply its frequency response by the function $a \cdot \mathrm{sinc}^2\ (\omega\ a/2)$ [21] .

Table 1 Frequency Response of Filter Functions

Filter	$\hat{\phi}(\omega)$	Ref.
Shepp-Logan	$\hat{\phi}_1 = \left\| \frac{2}{a} \sin\left(\frac{\omega a}{2}\right) \right\|$	[20]
Modified Shepp-Logan	$0.4\,\hat{\phi}_1 + 0.6\,\hat{\phi}_1 \cos(\omega a)$	[20]
Ramach.-Lakshmin.	$\hat{\phi}_2 = \frac{1}{a}\|\omega\|$ for $\|\omega\| \leq \frac{\pi}{a}$	[19]
	$= \frac{1}{a}\left\|\frac{2\pi}{a} - \omega\right\|$ for $\frac{\pi}{a} < \|\omega\| \leq \frac{2\pi}{a}$	
Modified Ramach.-Lakshmin.	$0.4\,\hat{\phi}_2 + 0.6\,\hat{\phi}_2 \cos(\omega a)$	proposed
Generalized $\|\omega\|$- filter	$\hat{\phi}_3 = \frac{1}{a}\|\omega\| \exp\left[-\xi\|\omega\|^p\right]$ for $\|\omega\| \leq \frac{\pi}{a}$	[21]
	$= \frac{1}{a}\left\|\frac{2\pi}{a} - \omega\right\| \exp\left[-\xi\left\|\frac{2\pi}{a} - \omega\right\|^p\right]$ for $\frac{\pi}{a} < \|\omega\| \leq \frac{2\pi}{a}$	

A comparisan of the frequency responses of the Shepp-Logan filter (rectified sine wave, SL), the modified Shepp-Logan filter (MSL), the Ramachandran-Lakshiminaryanan filter (triangular wave, RL) and some typical generalized $|\omega|$- filters are shown in Figs. 3-6. We propose to modify Ramachandran-Lakshiminaryanan filter (MRL), the same modification Shepp and Logan did to their own (see Fig.4). It is quite clear that the RL filter form has the best approximation of the function $|\omega|$, for $|\omega| \leq \frac{\pi}{a}$, while the SL filter has the smoothest response. Figure 6 introduces the fact that the generalized $|\omega|$-filter - through the proper choice of the parameters p and ξ - can fit any where in the gap between the RL and the MRL filter responses. The differences in behaviour of these filter functions are compared - in next section - through their performances in reconstructing specific simulated field functions.

COMPUTER SIMULATION AND DISCUSSION

The goals of such simulation are to test the performance of a limited angle tomographic technique on some specific fields, and to investigate the appropriateness of the filter functions (Table 1) to fluid flow and combustion applications . A Gaussian function, $F_1(x,y) = \exp\left[-10(x^2+y^2)\right]$, was tested. The choice of such functional form has been made because of its similarity to the fairly smooth concontration profiles of chemical species in diffusion flames for instance. A cylindrical function, $F_2(x,y) = 1$ for $x^2 + y^2 \leq 0.25$ had been reconstructed. This is because of its resemblance to point source or sharp discontinuity (as test section window or annulus secondary flow). In reconstructing both functions a value of M = 100 is chosen. The filter functions MRL, MSL and generalized

$|\omega|$-filter (with p=2.6 and $\xi = 10^{-5}$) are utlized. RL and SL filters were omitted because they show somewhat undesirable oscillations in the performed reconstructions.

Figure 7 gives the central slices of the reconstructed 40x40 Gaussian function F_1, using the convalution algorithm with three different functions (mentioned in last paragraph) at five different viewing angles N. Figures 7 and 9 indicate two significant characteristics of the algorithm. First with increasing the number of viewing angles N, the reconstruction will converge to approximately the true function. The selection of filter function had little effect on rms error and on image quality of F_1. A six -angle convolution technique gives 5.5 % accuracy with eith MSL or proposed MRL filter functions. Second, the choice made for the generalized filter parameters is not suitable for combustion diagnostics.

Figure 8 shows the central response of the technique to a uniform cylindrical function F_2. The previous three filter functions are atilized at five different projecting angles N. No significant differences between the reconstructions with MSL filter and the proposed MRL filter function (rms error). Figure 9 introduces the fact that there is no way of getting reasonable reconstructions of sharp changing property fields (as F_2) by using data from few views with convolution algorithm. The probable reason that the reconstruction of F_2 is not as good as that of F_1 is that the F_2 has larger bandwidth than the smoother F_1 [20].

CONCLUSION

From the results reported in this work, it has been shown that the proposed modification of the Ramachandran-Lakshminarayanan filter function will produce about the same response as that of the modified Shepp-Logan filter. Either one can be used with the six-angle convolution algorithm for reconstruction of axisymmetric low concentration and / or temperature fields in fluid flow and combusition processes (about 5.5% accuracy). More work has to be done for the proper choice of generalized filter parameters, to suit fluid flow and combustion diagnostics . The technique response-using different filters- to noise projections, and the problem of ray path bending have to be carefully checked.

ACKNOWLEDGEMENT

The auther is deeply indebted to Prof. R. Goulard at the George Washington University, Wash., D.C., for his valuable discussions, helpful suggestions and encourgements.

REFERENCES

1. Hartley, D.L., " Laser Scattering Diagnostics for Temperature and Concentration Measurements", AIAA Prog. Astro. and Aero., 53, 467-477 (1976).

2. Wang, C.D., " Laser Applications to Turbulent Reactive Flows", Comb. Sci. and Tech., 13,211-227(1976).

3. Schreiber, P.W., Gupta, R. and Roh,W.B., " Applications of Lasers to Combustion Diagnostics", Proc. SPIE, 158, 42-58(1978).

4. Lapp., M. and Soo, R.M., " The Study of Turbulent Diffusion Flames: Modeling Needs and Experimental Light Scattering Capabilities ", Proc. AGARD, Brussels (1980).

5. Lederman, S. and Sacks, S., "Laser Diagnostics for Flowfields, Combustion and MHD Applications", AIAA J., 22, 161-173 (1984).

6. Radon, J. ,"On the Determination of Functions from Their Integrals", Ber. Saechs. Akad. Wiss. Leipzig, Math-Phys., 262-277 (1917).

7. Bracewell, R.N., "Strip Integration in Radioastronomy", Aust. J. Phys., 9, 198-217 (1956).

8. Cromack , A.M., " Representation of a Function by Its Line Integrals, With Some Radiological Applications", J. Appl. Phys., 34, 2722-2727 (1963).

9. Hunsfield, G.N., " A Method of and Apparatus for Examination of a Body by Radiation Such as X-Ray", British Patent No. 1283915, London (1972).

10. Goulard, R. and Emmerman, P.J., "Absorption Diagnostics", Paper AIAA-79-85, 17th Aero. Sci, Meeting, New Orleans (1979).

11. Emmerman, P.J., " Application of Tomographic Reconstruction to Combustion and Fluid flow Diagnostics", D.Sc. Thesis, GWU, Wash.,D.C. (1980).

12. Goulard, R. and Emmerman, P.J., " Combustion Diagnostics by Multiangular Absorption", Curr. Phys. ,20 , 35-40 (1980).

13. Emmerman, P.J., Goulard, R., Santoro , R.J. and Samerjian, H.G., "Multiangular Absorption Diagnostics of a Turbulent Argon-Methane Jet", J. Energy, 4, 7o-77 (1980).

14. Ray, S. and Semerjian, H.G., "Laser Tomography for Temperature and Concentration Measurement in Reacting Flows", Presented at West. States Sec. / Comb. Inst., CA. (1982).

15. Goulard, R. and Ray, S., "Optical Tomography in Combustion and Meteorology", Presented at Workshop on Adv. in Remote Retriev. Methods, VA. (1984).

16. Worcester, P.F., " Remote Sensing of the Ocean Using Acoustic Tomography", Presented at Workshop in 15 .

17. Flemming, H.E., " Temperature Ratrievals Via Satellite Tomography", Presented at Workshop in 15.

18. Gordon, R., " A Tutorial on ART", IEEE Trans. on Nuclear Sci., NS-21, 78-93 (1974).

19. Ramachandran, G.N. and Lakshminarayanan, A.V., " 3-D Reconstruction from Radiographs and Electron Micrographs: Application of Convolution Instead of Fourier Transforms", Proc. Nat. Acad. of Sci. USA, 68, 2236-2240 (1971)

20. Shepp, L.A. and Logan, B.F., " The Fourier Reconstruction of a Head Section ", IEEE Trans. on Nuclear Sci., NS-21, 21-43(1974).

21. Kwoh, Y.S., Reed, I.S.and Truong. T.K., "A Generalized ω -filter for 3-D Reconstruction", IEEE Trans. on Nuclear Sci., NS-24, 1990-1998 (1977).

22. Hinze, J.O., "Turbulence", 2nd Ed., McGraw-Hill Co., New York (1975).

23. Yule, A.J., "Large Scale Structure in the Mixing of a Round Jet", J.

Fluid Mech., 89, 413-432 (1978).

24. Siegel, R. and Howell, J.R., " Thermal Radiation Heat Transfer", 2nd Ed. McGraw-Hill Co., New York (1981).

25. Swindall, W. and Barrett, H., " Computerized Tomography: Taking Sectional X-Rays", Phys. Today. 12,32-41 (1977).

26. Bracewell, R.N., " The Fourier Transform and Its. Applications", 2nd Ed., McGraw-Hill Co., New York (1978).

NOMENCLATURE

a	spacing between parallel beams
$F(x,y)$	Property field function = $Q_{\nu i}$ N_i
I_ν	Transmitted radiation intensity (at frequency ν)
$I_{\nu o}$	Incident laser intensity (at frequency ν)
M	Number of parallel rays per projection
N	Number of viewing angles
N_i	The ith species concentration
$P(r,\theta)$	Projection of $F(x,y)$ at angle θ
p	Switch parameter (for generalized filter), $p \geq 0$
$Q_{\nu i}$	Absorption cross section of ith species (at frequency ν)
R	Radius of the property field
r	Radial coordinate
S_r	Sampling rate
s	Absorption path length
x,y	Cartesian coordinates
η	Dummy variable
θ	Viewing angle
ν	incident light frequency
ξ	Damping factor (for generalized filter), $\xi \geq 0$
ρ	Spatial frequency (in the transform domain)
ρ_{max}	Spatial frequency bandlimit
τ	Dummy variable
$\phi(r)$	Filter function
ω	$2\pi\rho$
λ	Denotes Fourier transform operation

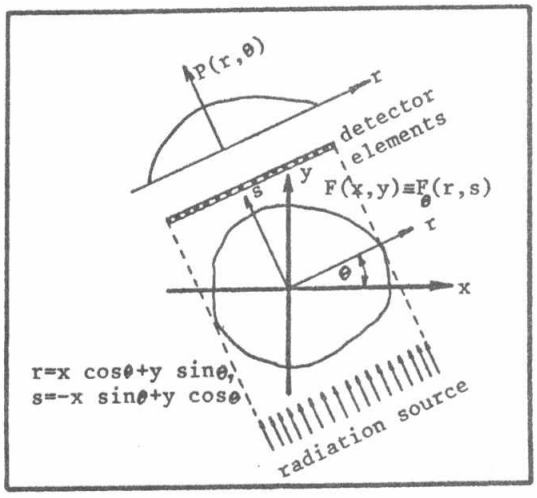

Fig.1. An object $F(x,y)$ and its projection $P(r,\theta)$ in the spatial domain.

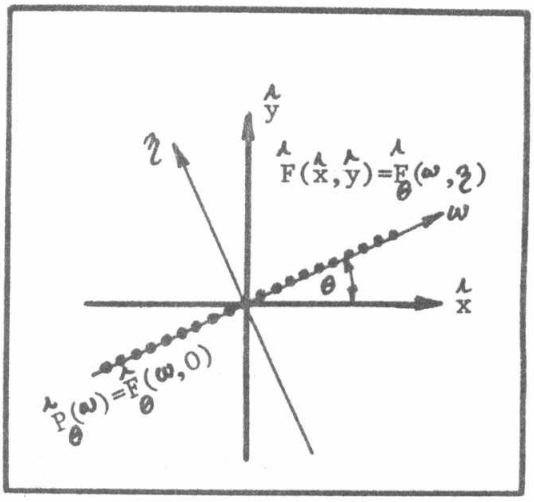

Fig.2. The function $\hat{F}(\hat{x},\hat{y})$ in the frequency domain.

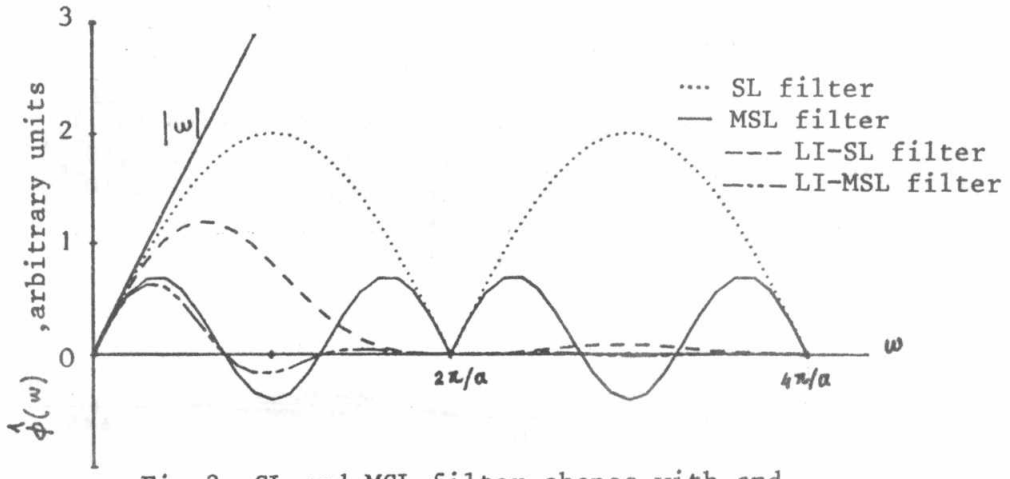

Fig.3. SL and MSL filter shapes with and without linear interpolation.

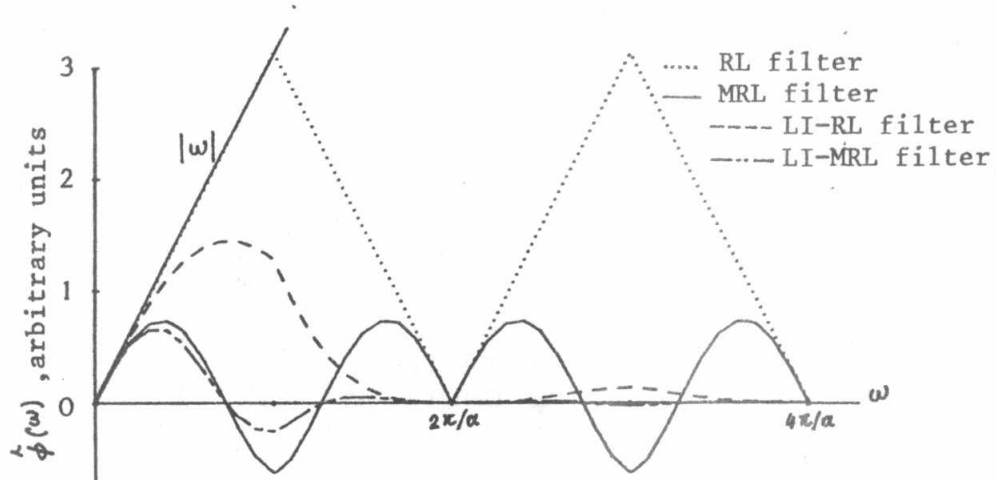

Fig.4. RL and MRL filter shapes with and without linear interpolation.

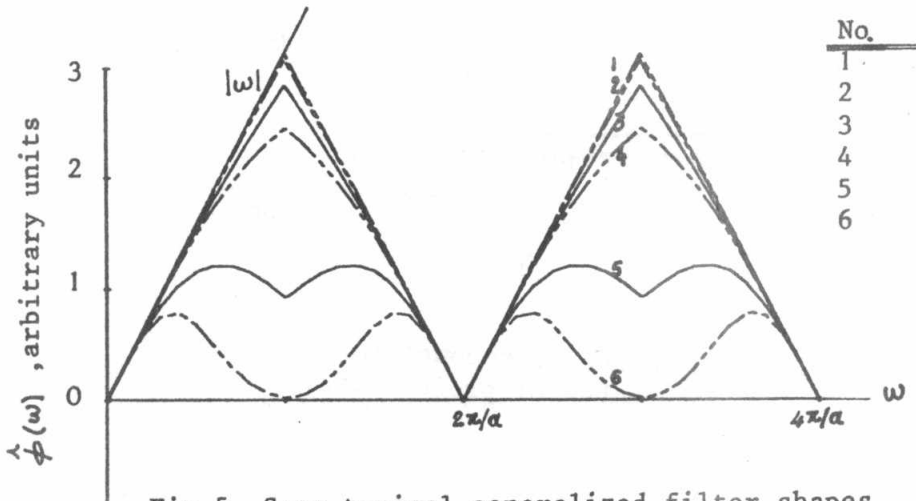

No.	p	$\xi \times 10^5$
1	1	1
2	1.5	1
3	1.5	5
4	2	1
5	2	5
6	2.6	1

Fig.5. Some typical generalized filter shapes without linear interpolation.

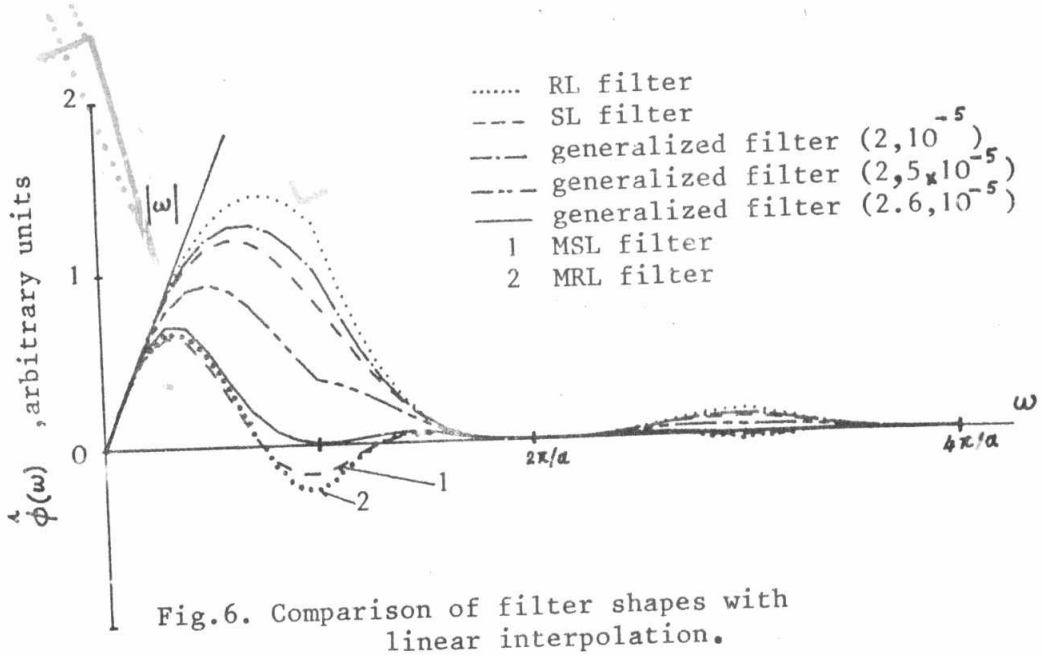

Fig.6. Comparison of filter shapes with linear interpolation.

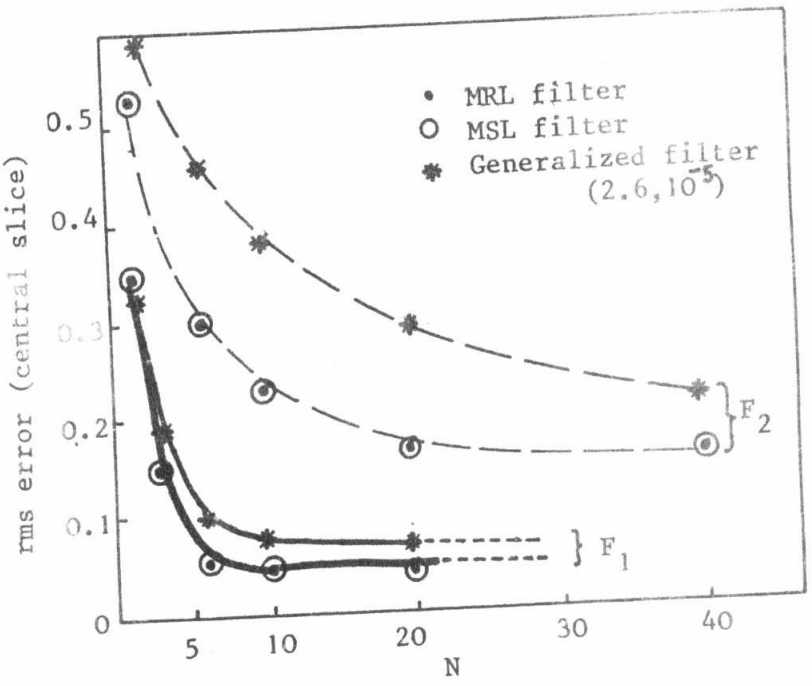

Fig.9. Dependence of reconstruction accuracy on number of projections.

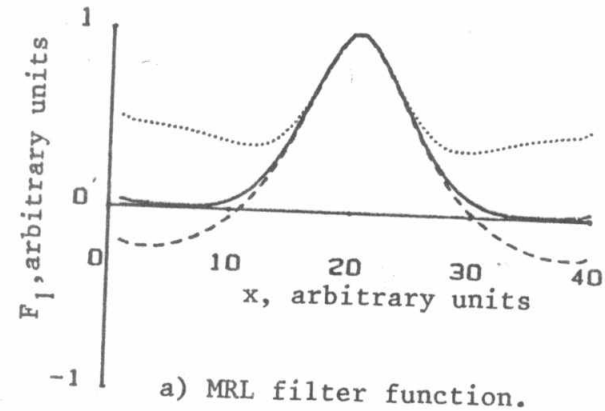

a) MRL filter function.

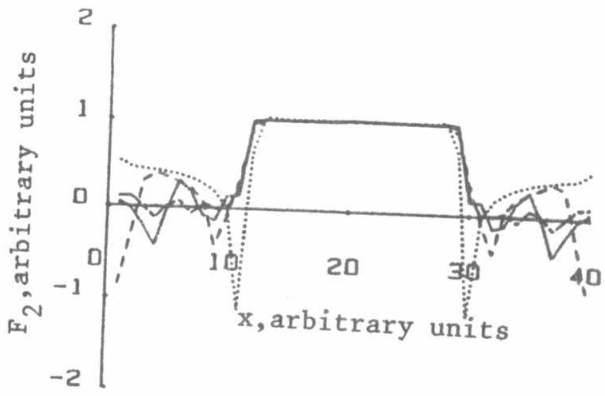

a) MRL filter function

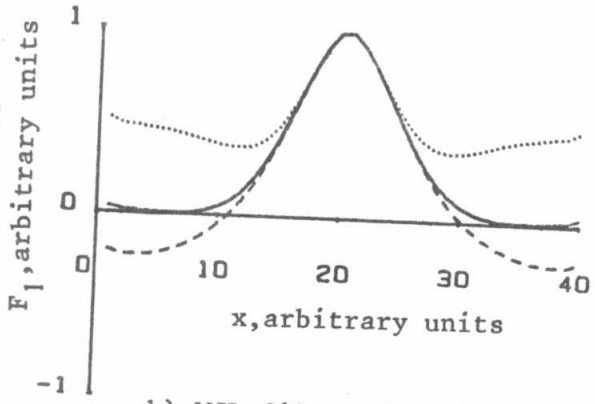

b) MSL filter function.

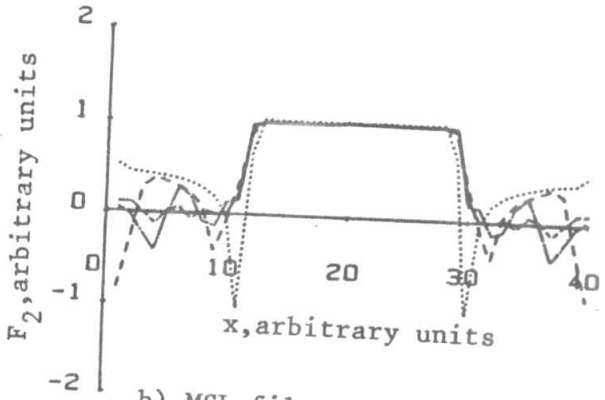

b) MSL filter function

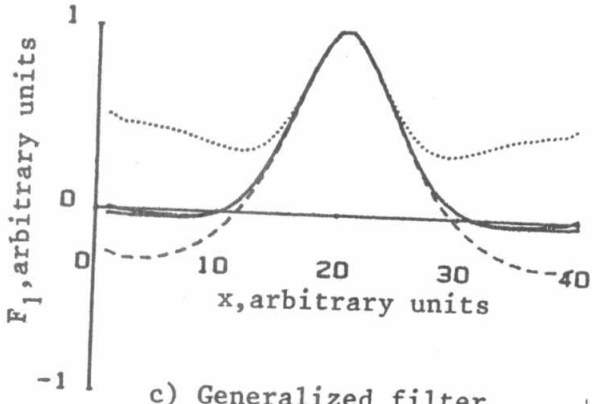

c) Generalized filter $(2.6, 10^{-5})$

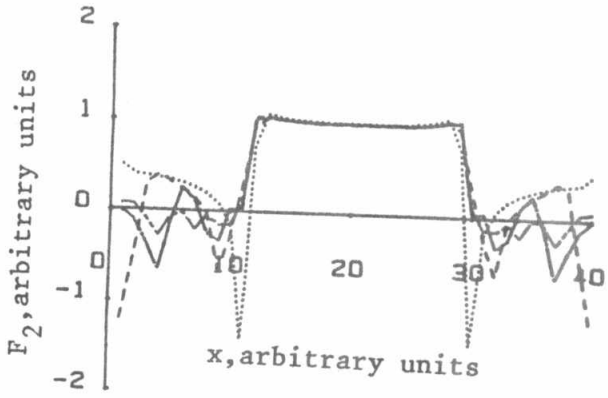

c) Generalized filter $(2.6, 10^{-5})$

Fig.7. Central slices through the reconstruced Gaussian function F_1 using three filter functions with five different viewing angles (··· N=2, --- N=3, —·— N=6, —··— N=10 and —— N=20).

Fig.8. Central slices through the reconstructed uniform cylindrical function F_2 using three filter functions with five different viewing angles (··· N=2, --- N=6, —·— N=10, —··— N=20, and —— N=40).